Proceedings of ERAD (2002): 25–30 © Copernicus GmbH 2002

ERAD 2002

# Error analysis of a polarimetric dealiasing technique for Doppler measurements of the atmosphere

**C. M. H. Unal**[1] **and D. N. Moisseev**[2]

[1]IRCTR (International Research Centre for Telecommunications-transmission and Radar), Faculty of Information Technology and Systems, Delft University of Technology, 2628 CD Delft, NL
[2]Physical, Geometric and Space Geodesy Section, Faculty of Civil Engineering and Geosciences, Delft University of Technology, 2628 CD Delft, NL

**Abstract.** Performing simultaneously Doppler and polarimetric measurements can result in a better description of atmospheric targets. The output of this Doppler polarimetric measurement is a covariance matrix per Doppler bin. Two difficulties for these measurements were encountered. The first one is the non-simultaneity of the polarimetric measurements, which is solved by a phase correction per Doppler velocity bin, valid in case of Doppler aliasing. The second problem is the reduction of the maximum unambiguous Doppler velocity due to the transmission of different polarizations, which is solved by a new dealiasing technique using the phase of the cross spectrum $hh, vv$. In order to elaborate a dealiasing algorithm, a statistical model of the phase of the cross spectrum $hh, vv$ is introduced and experimentally verified to obtain the standard deviation of this phase for different measurement conditions (number of averages, cross correlation coefficient). The dealiasing procedure is then discussed and illustrated on a slant profile of light precipitation measured during a windy day. An advantageous consequence of this procedure, which is ground clutter suppression, is also pointed out. Comparison of the obtained dealiased Doppler velocities is carried out using a meteorological balloon.

## 1 Introduction

The use of radar polarimetry for weather surveillance improves hydrometeors recognition and classification (Zrnic and Ryzhkov, 1999). The polarimetric content of the radar signal is expressed by a target covariance matrix, which describes the mean polarimetric properties of the hydrometeors. Well-known polarimetric meteorological parameters, like the differential reflectivity $Z_{dr}$ and the complex cross correlation coefficient $\rho_c$ are derived from this matrix. With the two $S$-band coherent polarimetric radars at our disposal, TARA (Transportable Atmospheric RAdar) and DARR (Delft Atmospheric Research Radar), we aim at measuring and interpretating the Doppler spectrum of these polarimetric meteorological parameters. For example, in the case of rain in absence of turbulence, the differential reflectivity (sensitive to the shape of the raindrops) is calculated for each Doppler velocity bin (related to the size of the raindrops) and this may lead to the shape-size relationship. Other polarimetric meteorological parameters, like the linear depolarization ratio, the complex cross correlation coefficient are also available for all the Doppler velocity bins considered. From these measurements (Doppler polarimetric), we expect to obtain more detailed information about the microphysical properties of the hydrometeors. Prior to the interpretation, a correct processing of the spectral target covariance matrix (Doppler spectra of the elements of the target covariance matrix) must be carried out. This paper is related to two measurement and processing problems: non simultaneity of the polarimetric measurements and Doppler aliasing. A solution to these two problems is given in (Unal and Moisseev, 2002) where it is shown that the proposed phase compensation is a valid correction for the non simultaneity of the polarimetric measurements in case of Doppler aliasing and that it leads to a new possiblity for dealiasing precipitation profiles. These results are briefly summarized in this paper. The focus of this paper is on the error analysis of the proposed methods, especially for the new dealiasing technique. The performance of these techniques is analysed for different measurement scenarios, special attention is given to the measurements of rain, clouds and melting layer of light precipitation.

*Correspondence to:* C. M. H. Unal
(c.m.h.unal@its.tudelft.nl)

## 2 Correction for the non simultaneity of the polarimetric measurements

The Doppler polarimetric measurement consists of time series of the elements of the scattering matrix. Doppler processing is carried out on these time series and a covariance matrix is calculated per Doppler velocity bin.

The proposed correction is a phase compensation per

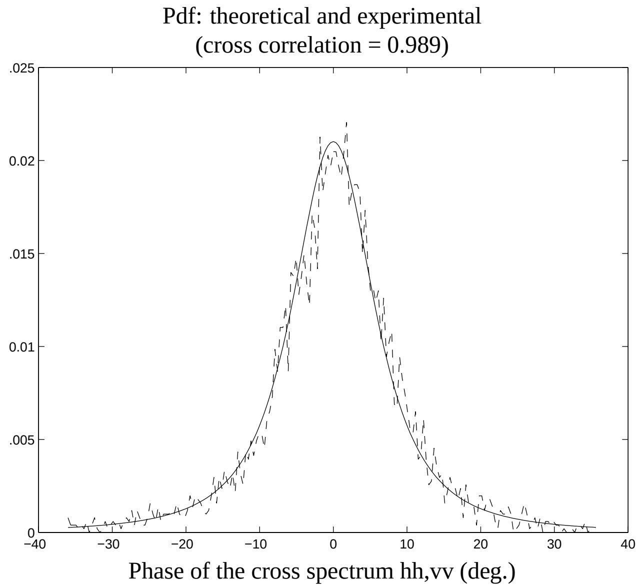


**Fig. 1.** Probability density functions of the cross spectrum phase (no average.)

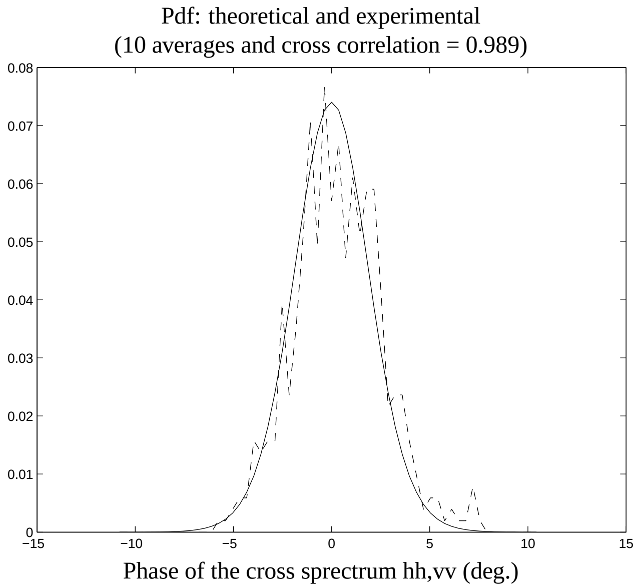


**Fig. 2.** Probability density functions of the cross spectrum phase (10 averages.)

Doppler bin. It is called Doppler phase compensation and is only relevant for the cross spectra of the scattering matrix. In the paper, we focus on the cross spectrum $hh, vv$

$$F_{hh,vv} = \langle \hat{S}_{hh} \hat{S}^*_{vv} \rangle \tag{1}$$

The symbol ˆ indicates that the second moments of the scattering matrix $[S]$ are expressed in the Doppler domain. They depend on the range bin and on the Doppler bin. The symbol $<>$ means time average.

For light precipitation, the differential phase $\Psi_{DP}$ is expected to be near 0° at $S$-band. When this phase is obtained per Doppler bin, it is then the argument of the cross spectrum $F_{hh,vv}$. For Doppler velocities $v_D$ inferior to the maximum unambiguous Doppler velocity $v_{D,max}$ (in magnitude), the phase of the cross spectrum, without Doppler phase compensation, is

$$\begin{aligned} Arg\left(F_{hh,vv}\right) &\approx \Psi_{DP}\left(v_D\right) + \frac{4\pi}{\lambda} v_D \Delta t \\ &= \Psi_{DP}\left(v_D\right) + \Delta\phi_D \end{aligned} \tag{2}$$

where $\Delta t$ is the time offset between $hh$ and $vv$ measurements. For a vertical profile of rain, the decorrelation time and $\Delta t$ are typically 10 ms and 1 ms, respectively. The phase of the cross spectrum will vary between $\Psi_{DP}$ and $\Psi_{DP}$ + $2\pi/10$. For slant profiles, which are affected by the wind Doppler velocity, this error on the differential phase will be larger. After adding the phase

$$\Delta\phi^c_D = -\Delta\phi_D \tag{3}$$

per Doppler bin, the Doppler phase compensation is performed and the phase spectrum becomes

$$Arg\left(F^c_{hh,vv}\right) \approx \Psi_{DP}\left(v_D\right) \tag{4}$$

For Doppler velocities larger in modulus than the maximum unambiguous Doppler velocity, the corresponding measured Doppler velocities are

$$v^m_D = v_D \mp 2v_{D,max} \tag{5}$$

with $-$ for $v_D$ belonging to the interval $]v_{D,max}, 3v_{D,max}]$ and $+$ for $v_D$ belonging to the interval $]-3v_{D,max}, -v_{D,max}]$. Before Doppler phase compensation the Eq. (2) holds and after the Doppler phase compensation, which consists of adding the phase

$$\begin{aligned} \Delta\phi^c_D &= -\frac{4\pi}{\lambda} v^m_D \Delta t = -\Delta\phi_D \pm \frac{8\pi}{\lambda} v_{D,max} \Delta t \\ &= -\Delta\phi_D \pm \Delta\phi_{D,max} \end{aligned} \tag{6}$$

the phase spectrum becomes

$$\begin{aligned} Arg\left(F^c_{hh,vv}\right) &= \Psi_{DP}\left(v_D\right) \pm \Delta\phi_{D,max} \\ &= \Psi_{DP}\left(v_D\right) \pm 2\pi \frac{\Delta t}{T_m} \end{aligned} \tag{7}$$

where $T_m$ is the sampling time for the Doppler FFT.

The Doppler phase compensation is correctly performed in the case of Doppler aliasing but then a constant phase is added to the cross spectrum.

In case of multiple Doppler aliasing, the Eq. (7) can be generalized. We use a cycle of three polarimetric measurements, $hh$, $hv$ and $vv$ because of the single receiver channel of the radar. Therefore, $\Delta t = 2T_m/3$ which leads to the generalized form

$$Arg\left(F^c_{hh,vv}\right) \approx \Psi_{DP}\left(v_D\right) \pm n_D \frac{4\pi}{3} \tag{8}$$

When $\Psi_{DP}$ is near 0, we obtain phase ambiguity from $n_D = 3$ and we can solve two different aliasing problems.

## 3 Statistical model of the cross spectrum phase

A new dealiasing technique based on the phase of the cross spectrum $hh, vv$, which was discussed in Sect. 2, will be explained and illustrated in Sect. 4. After correction for the non simultaneity of the polarimetric measurements $hh$ and $vv$, the mean value of this phase is 0 for light precipitation at $S$-band (see the probability density function of the measured phase of the cross spectrum $hh, vv$, in Figs. 1–2, dashed line). It was shown in Sect. 2 that this value becomes a specific constant ($\pm 2\pi\Delta t/T_m$) in the presence of a single Doppler aliasing. In order to develop a dealiasing algorithm, it is necessary to know the standard deviation of this phase and its dependency on the number of averages. For this purpose, a statistical model of the phase of the cross spectrum is hereby introduced and experimentally verified.

When many hydrometeors are contained in the radar resolution volume (range bin) or in a part of this radar resolution volume (range-Doppler bin) and no single one of them dominates the others, the scattering matrix can be modeled as having a multivariate complex Gaussian distribution. With this assumption, a probability density function

$$p^k(\psi) = \frac{\Gamma\left(k+\frac{1}{2}\right)\left(1-|\rho_c|^2\right)^k \beta}{2\sqrt{\pi}\Gamma(k)\left(1-\beta^2\right)^{k+\frac{1}{2}}} + \frac{\left(1-|\rho_c|^2\right)^k}{2\pi} F\left(k, 1, \frac{1}{2}; \beta^2\right) \quad (9)$$

for the phase

$$\psi = Arg\left[\frac{1}{k}\sum_{i=1}^{k} S_{hh}(i)\, S_{vv}^*(i)\right] \quad (10)$$

is given by (Lee, 1994). This phase is comprised between $-\pi$ and $\pi$ and the probability density function depends on the complex cross correlation coefficient

$$\rho_c = \frac{E\left[S_{hh}S_{vv}^*\right]}{\sqrt{E\left[|S_{hh}|^2\right]}\sqrt{E\left[|S_{vv}|^2\right]}} = |\rho_c| e^{j\Psi_{DP}} \quad (11)$$

and on the number of averages $k$. The parameter $\beta$ is defined as follows

$$\beta = |\rho_c| \cos\left(\psi - \Psi_{DP}\right) \quad (12)$$

and the functions $\Gamma$ and F (more precisely ${}_2F_1$) are the gamma function and the Gauss hypergeometric function, respectively. The complex cross-correlation coefficient depends on meteorological conditions (for heavy precipitation, $\Psi_{DP}$ will be different from 0 and the modulus of $\rho_c$ may decrease).

The phase of the cross spectrum $hh, vv$ is

$$\psi(l) = Arg\left[\frac{1}{k}\sum_{i=1}^{k} \hat{S}_{hh}(i,l)\, \hat{S}_{vv}^*(i,l)\right] \quad (13)$$

where $l$ denotes the Doppler bin. This phase corresponds to the differential phase per Doppler velocity bin after $k$ averages. Because heavy precipitation are very scarce in The Netherlands (moderate climate), we use rather the differential phase to reveal measurement problems like Doppler aliasing or ground clutter than to characterize hydrometeors.

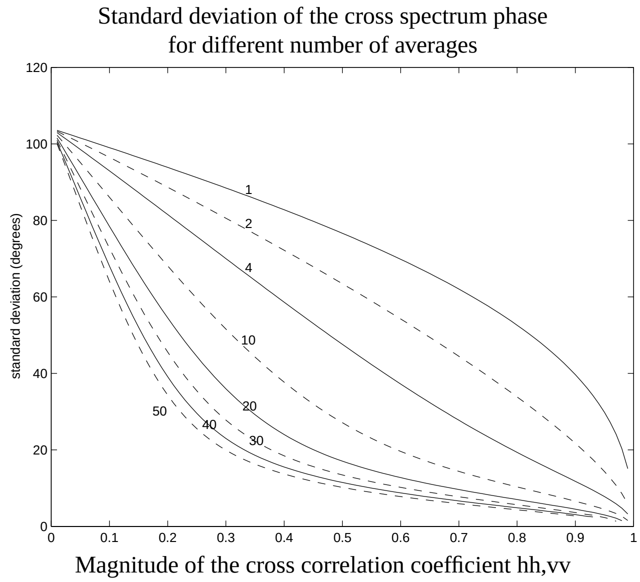


**Fig. 3.** Standard deviation of the cross spectrum phase.

An estimate of the magnitude of the cross correlation coefficient per Doppler bin is obtained using 40 averages in the case of a vertical profile of precipitation. The rain and precipitating cloud areas show high values of this parameter, typically 0.99 and we find maximally 0.97 in the melting layer. These values are characteristic of stratiform light rain. We first verify that the number of averages considered (40) consists of independent samples. This is the case when we look at time series of the cross spectrum phase and its corresponding autocovariance function. We verify then that this phase distribution is a good model for our experimental data in Figs. 1–2. The probability density functions, theoretical and experimental, are plotted for a cross correlation 0.989 with no average (Fig. 1) and 10 averages (Fig. 2). The experimental normalized histogram corresponding to 10 averages is built with 10 times less data than the one with no average. Nevertheless we can conclude that there is a good fit between the theoretical and experimental probability density functions, with or without average.

Since the model of the cross spectrum phase distribution is verified, the related standard deviation

$$\sigma_\psi(k) = \sqrt{\frac{\int_{-\pi}^{\pi} \psi^2 p^k(\psi)\, d\psi}{\int_{-\pi}^{\pi} p^k(\psi)\, d\psi}} \quad (14)$$

can be computed versus the magnitude of the cross correlation coefficient for several number of averages. This is plotted in Fig. 3. After Doppler processing, the cross correlation coefficient is generally comprised between 0.9 and 1 for light precipitation. In that case, the largest standard deviation, about 40°, is obtained for $|\rho_c|$ = 0.9 when there is

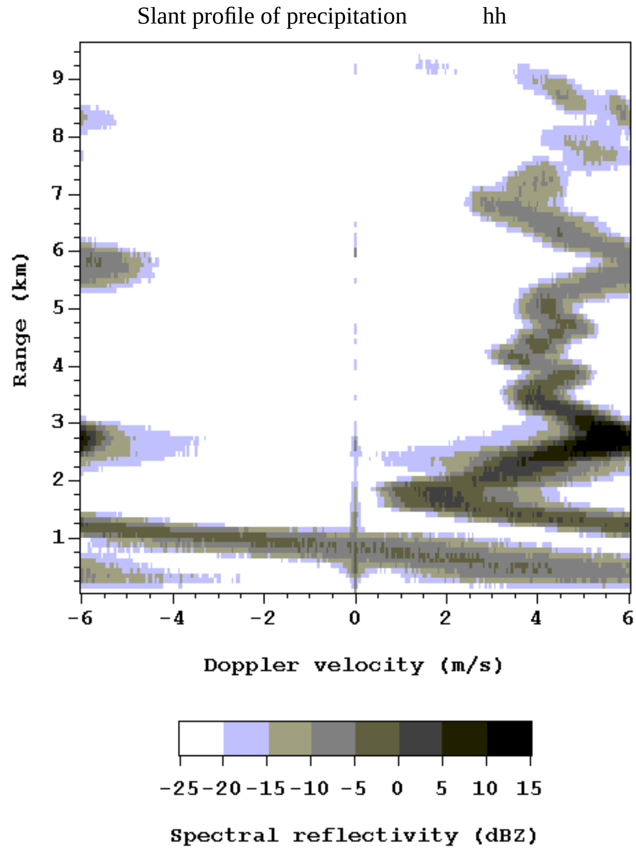


**Fig. 4.** Spectral reflectivity of a slant profile.

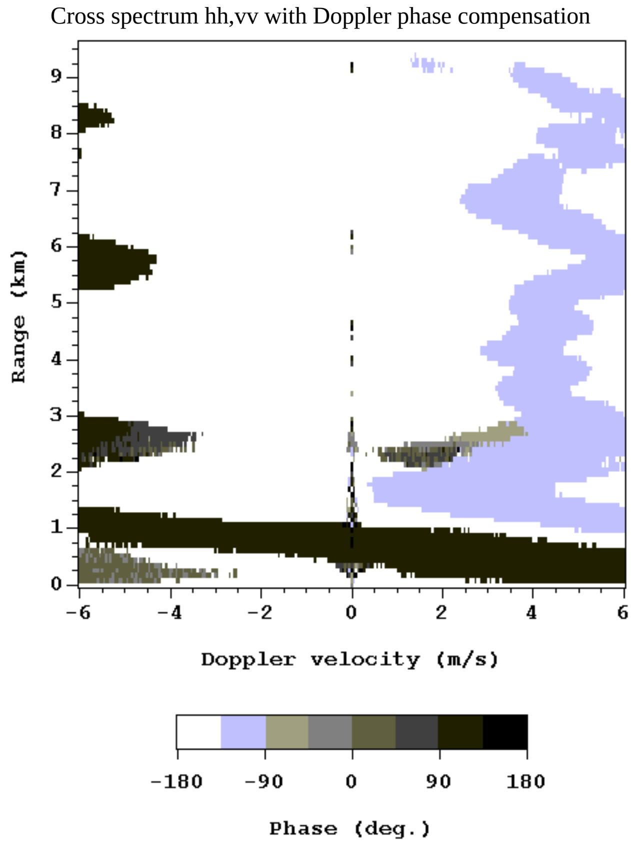


**Fig. 5.** Compensated cross spectrum phase.

no average. When there is a single aliasing, the mean phase is 120° (with our measurement specifications), which indicates that the highest standard deviation possible is 60° before phase ambiguity occurs. Therefore a dealiasing technique based on the cross spectrum phase can be successfully used when there is no average. Nevertheless, Fig. 3 shows that it is worthwhile to carry out an average on two Doppler spectra, which leads to a strong reduction of the standard deviation, which becomes about 20°. For the same example (no average and $|\rho_c|$ = 0.9), the mean $\Psi_{DP}$ may reach maximally 20°.

## 4 Dealiasing procedure

### 4.1 Slant profile of precipitation

To illustrate the dealiasing procedure, a slant profile (Fig. 4) is selected. It shows light stratiform precipitation at $hh$ polarization. The radar looks at an elevation angle of 30°. The range resolution is 75 m. The melting layer is located between the ranges 2 km and 3.1 km. Under the melting layer, there is rain. The precipitating cloud layer is located between the ranges 3.1 km and 9.25 km. The Doppler resolution is 4.71 cm/s. The negative Doppler velocities indicate that the hydrometeors are approaching the radar. The measurements are carried out with the maximum Doppler velocity being too low. For slant profiles, the Doppler velocities cannot be related directly to the fall speed of the hydrometeors and contain the wind Doppler velocity. The selected slant profile shows large variations in wind Doppler velocity as a function of height in Fig. 4, especially in the rain area.

### 4.2 Dealiasing of the slant profile

The phase of the cross spectrum $hh, vv$ is plotted in Fig. 5 after Doppler phase compensation. Three phase values are mainly seen. The dark gray area is the only part of the precipitation event, rain in the near range, which belongs to the Doppler velocity interval [−6., +6.]. The phase of the cross spectrum is about 0°. This precipitation measurement shows two other characteristic phases: one is about 120° (nearly black) and the other one is about −120° (light gray). These values indicate the presence of Doppler aliasing and make it possible to retrieve to which Doppler interval they belong. In the example of the slant profile, the Doppler velocities are expected to be negative (the mean Doppler velocities per range bin calculated from the Doppler spectrum part related to the phase value 0° are near −6 m/s). When the precipitation event corresponds to the Doppler velocities interval [−18 m/s, −6 m/s], the constant phase $-4\pi/3$ is added to the phase of the cross spectrum $hh, vv$. This constant phase

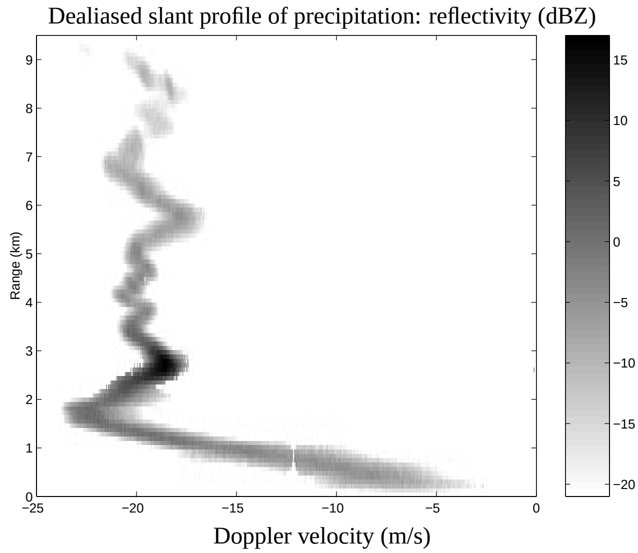


**Fig. 6.** Dealiased slant profile: spectral reflectivity.

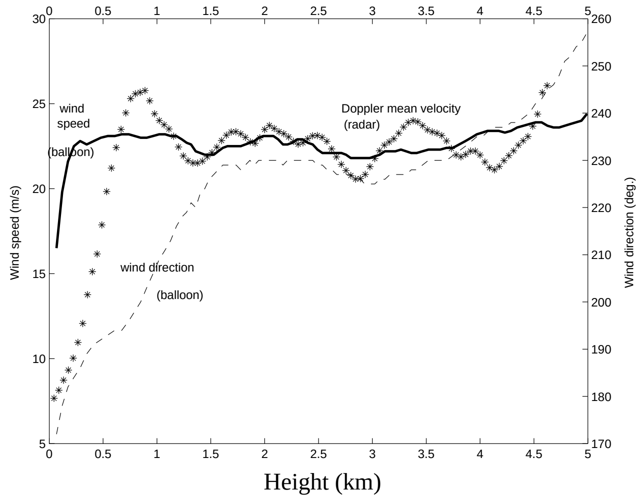


**Fig. 7.** Radio sonde and radar measurements: wind profiles.

is $-240°$ or equivalently $120°$ and corresponds to the nearly black area. The same occurs for velocities belonging to [$-30$ m/s, $-18$ m/s], then the constant phase $-8\pi/3$ is added to the cross spectrum phase and leads to the light gray area $-480°$ or equivalently $-120°$.

Using the phase of the cross spectrum and continuity of the mean Doppler velocity, the dealiased slant profile is given in Fig. 6. The number of averages is 50 for this event. Only the areas corresponding to a cross correlation larger than 0.7 and having a cross spectrum phase comprised in the interval (mean phase) $\pm 2\sigma_\psi$ have been considered. The largest standard deviation $\sigma_\psi$ is 6° and three mean phases are found. For this example, the mean $\Psi_{DP}$ may reach 6°. The standard deviation can be chosen larger in order to allow for a larger mean $\Psi_{DP}$ than 6°.

## 4.3 Consequences of the dealiasing procedure

The phase of the cross spectrum $hh, vv$ also indicates problematic zones because of the presence of very different phase values than expected. Two examples of them, present in Fig. 5, are shortly discussed: ground clutter and melting layer.

The cross spectrum phase is very useful to detect the Doppler cells contaminated by the ground clutter. After removal of the stable ground clutter, the time varying ground clutter shows a broad histogram of phases (see Fig. 5 around the Doppler velocity 0 m/s). Therefore during the dealiasing procedure (also if the threshold on the magnitude of the cross correlation coefficient is not applied), the Doppler cells significantly affected by ground clutter are discarded and that can be seen in Fig. 6, under and above 1 km in the rain area (missing data around Doppler velocity $-12$ m/s). We can conclude that this dealiasing technique performs dealiasing of the precipitation profile and ground clutter suppression.

In the second area, the proposed dealiasing technique may not perform optimally. This is the melting layer (between 2 and 3 km). Under the reflectivity peak of the melting layer (2.75 km), the Doppler spectra become wide (2.5 km). In the tail of these Doppler spectra, the reflectivity values are similar to those of a precipitating cloud but the cross correlation coefficient magnitude is small and the cross spectrum phase differs from expectations. At the present moment, the dealiasing procedure suppresses the tails of these Doppler spectra. This effect can be clearly seen for a few range bins at 2.2 km in the dealiased profile of Fig. 6. These Doppler spectra in the lower part of the melting layer (under the reflectivity peak) are being investigated.

## 4.4 Comparison with a meteorological balloon

In order to compare the Doppler velocities obtained after dealiasing the slant profile, one vertical profile of the wind conditions (balloon in Fig. 7) was kindly supplied by the Netherlands Meteorological Institute (KNMI). The two sensors are not collocated but a comparison can still be done. The mean velocity measured by the balloon (thick line) is mainly comprised between 22 m/s and 23 m/s from 0.2 km to 4.5 km (height). The estimated horizontal wind mean velocities, calculated for a vertical profile, are also plotted in Fig. 7 (asterisk). They correspond to the Doppler mean velocities of the slant profile divided by cos(30°), which means that the contribution of the hydrometeors to the Doppler mean velocity is here neglected. Apart from the first 0.5 km (range 1 km in the slant profile) there is a good agreement for the estimated wind velocities measured by the radar if the azimuth direction of the radar is near the horizontal wind direction (dashed line).

## 5 Conclusion

The solution to the non simultaneity of the polarimetric measurements, $hh$ and $vv$ is a phase correction per Doppler velocity bin (Doppler phase compensation), which is valid in the case of Doppler aliasing. This phase correction, which improves with the Doppler resolution, is general and can be applied for all moving targets. For atmospheric targets, this phase correction is necessary for the estimate of the complex cross correlation coefficient.

After Doppler phase compensation and in case of no Doppler aliasing, the phase histogram of the cross spectrum $hh, vv$ (or equivalently histogram of the differential phase per Doppler velocity bin) has a mean phase of $0°$ for light precipitation at $S$-band.

The Doppler phase compensation corrects for the non simultaneity of the polarimetric measurements in case of Doppler aliasing but adds a constant phase, which depends on the interval of the actual Doppler velocities. Thus dealiasing of the Doppler profiles can be done using the phase of the cross spectrum $hh, vv$. In the case of mean $\Psi_{DP}$ values significantly different from 0 (heavy precipitation), the same strategy can be used because this large and known jump in the phase of the cross spectrum $hh, vv$ at a fixed range, due to aliasing, can be easily detected.

In order to develop a dealiasing algorithm, it is necessary to know the standard deviation of this phase and its dependency on the number of averages. For this purpose, a statistical model of the phase of the cross spectrum is introduced and experimentally verified. The standard deviation is computed versus the magnitude of the cross correlation coefficient for several number of averages. After Doppler processing, the cross correlation coefficient is generally comprised between 0.9 and 1 for atmospheric targets like rain, melting layer and precipitating cloud. Therefore a dealiasing technique based on the cross spectrum phase can be successfully used when there is no average. Nevertheless, it is worthwhile to carry out an average on two Doppler spectra, which leads to a strong reduction of the standard deviation.

We have shown that the new dealiasing method, which is proposed, compensates for the reduction of the maximum unambiguous Doppler velocity in case of polarimetric measurements of light precipitation at $S$-band (assumption: mean $\Psi_{DP}$ small) and performs clutter suppression. This new dealiasing technique can be extended when large mean values of $\Psi_{DP}$ are encountered. In that case, the absolute values of the cross spectrum phase $hh, vv$ must not be considered but the jump of this phase in the Doppler spectrum at a fixed range.

## References

Lee, J.-S., K. W. Hoppel, S. A. Mango, and A. R. Miller, "Intensity and phase statistics of multilook polarimetric and interferometric SAR imagery," IEEE Trans. On Geoscience and Remote Sensing, vol. 32, no. 5, pp. 1017-1027, September 1994.

Unal, C. M. H. and D. N. Moisseev, "Improved Doppler processing for polarimetric radars: application to precipitation measurements," in Symposium on Propagation and Remote Sensing, URSI Commission F, Garmisch-Partenkirchen, (Garmisch-Partenkirchen, Germany), 2002.

Zrnic, D. S. and A. V. Ryzhkov, "Polarimetry for weather surveillance radars," Bulletin of the American Meteorological Society, vol. 80, no. 3, pp. 389-406, March 1999.